Resolution limitation of travel time tomography: beyond the first Fresnel zone

Cuiping Li[1], Neb Duric[1,2]

[1]Delphinus Medical Technologies, 46701 Commerce Center Drive, Plymouth, MI 48170; Email: cli@delphinusmt.com
[2]Karmanos Cancer Institute, 4100 John R. Street, 4 HWCRC, Detroit, MI 48201

ABSTRACT

Previous studies concluded that the resolution limitation of travel-time tomography is the width of the first Fresnel zone. However, we believe that the resolution of ray tomography cannot simply be limited to the first Fresnel zone and is affected by many factors. In this study, we investigate a variety of factors that affect the resolving power of travel time tomography. These factors include accuracy of picked travel time, ray coverage (data density) and data signal-to-noise ratio (SNR). We also investigate to what extent that bent-ray travel-time tomography is capable of resolving anomalous objects smaller than the first Fresnel zone based on numerical simulations. We have shown that bent-ray travel-time tomography resolvability and detectability of small objects is better than the first Fresnel zone.

Keywords: bent-ray travel time tomography, wave propagation, resolvability, detectability

1. INTRODUCTION

Ray theory based travel-time tomography plays a central role in ultrasound medical imaging because of its robustness. It is currently employed by our ring shaped breast ultrasound scanner to study suspicious breast masses. By taking ray bending into consideration, bent-ray ultrasound tomography can be used to generate more accurate sound speed images of breasts than straight ray tomography. Ray theory represents asymptotic high-frequency approximation of the propagating signal. In the ray method, ray path can be interpreted as a trajectory along which the high frequency part of the signal energy propagates from source to receiver. Ray theory ignores the influence of structures near the ray path due to the finite bandwidth of the propagating signal. The volume around the ray path that affects the first half-cycle of the wavefield at receiver is called the first Fresnel zone[1]. The Fresnel zone associated with the dominant frequency is commonly cited in the literature as the resolution limit of travel-time tomography[2-10]. This leads to the question: how confident are we to make an interpretation of those small findings in the reconstructed breast images? This question remains unanswered for the bent-ray ultrasound tomography. Yet, it is a critical consideration in the medical field where there is little room for error in diagnostic imaging.

In the previous studies, researchers believe that objects smaller than the first Fresnel zone are hidden due to the healing of the wave fronts that have diffracted around the object[2-10]. The theory of wave front healing was phrased by Pritchett[11] as "The concept of this theory is that wave fronts perturbed by inhomogeneities near the source will tend to heal and straighten out by diffraction as the wave front propagates farther from the source". Nolet et al. used Fresnel zone to investigate the loss of resolving power due to wave front healing[2]. Sneider et. Al[4] discussed the validity criteria of ray theory. Hung et al.[7] studied the resolution limitation of travel time tomography assuming that the travel time data was measured with cross-correlation method. In Williamson's paper[12], he investigated the straight-ray tomography to sound speed model of small perturbations to a constant background sound speed with monochromatic illumination. He showed that the resolution for such a special case is in the order of the width of the first Fresnel zone. However, Williamson also mentioned in his paper that for bent-ray tomography, larger perturbation and broad-band data, the resolution limit of travel-time tomography is less clear and needs further investigation[12].

In this paper, we calibrate a bent-ray travel-time tomography algorithm to address the resolution issue. For algorithm calibration, *in vivo* data are not appropriate because we don't know the truth ahead of time and breast phantom data

are limited because they can test only a limited set of parameters. Hence synthetic simulations are needed to fully understand the limitations of the tomography inversion. In this study, we investigate a variety of factors that affect the resolving power of travel time tomography. These factors include accuracy of picked travel time, ray coverage (data density) and data signal-to-noise ratio (SNR). We also investigate to what extent that bent-ray travel-time tomography is capable of resolving anomalous objects smaller than the first Fresnel zone based on numerical simulations. We have shown that bent-ray travel-time tomography resolvability and detectability of small objects is better than the first Fresnel zone.

2. MATERIALS AND METHODS

2.1 Bent-ray ultrasound tomography

Ultrasound rays in inhomogeneous medium (such as breast tissue) are bent based on Fermat's Principle and Snell's Law.

Let δt_i be the difference between the *ith* picked time-of-flight for the recorded ultrasound data and the *ith* calculated first arrival time for the soundspeed model, the bent-ray travel-time tomography problem can be described as follows

$$\sum_{j}^{M} l_{ij} \Delta s_j = \Delta t_i , \tag{1}$$

where Δs_j is the slowness perturbation for the *jth* grid cell, which needs to be inverted, and l_{ij} is the ray length of the *ith* ray within the *jth* cell. This is a nonlinear inverse problem due to ray bending and an iterative method is used to solve it. Reference[13] provides more details on how to solve equation (1).

In this study, we applied bent-ray travel-time tomography to the numerical simulations and we analyzed a variety of factors affecting the resolving power of bent-ray travel-time tomography.

2.2 The first Fresnel zone

The region of the first Fresnel zone is defined by the following condition[14]:

$$|T(S,F) + T(F,R) - T(S,R)| < TT/2. \tag{2}$$

Here *TT* is the period of the prevailing signal, *S* and *R* denotes the source position and receiver position, respectively, *F* is an auxiliary point in the vicinity of the ray path R-S, *T(S,F)* is the travel time for waves to propagate from *S* to *F*, similarly *T(F,R)* is the travel time for waves to travel from *F* to *R*, and *T(S,R)* is the travel time for waves to travel from *S* to *R* along an asymptotic ray path. The point *F* belongs to the first Fresnel zone if and only if it satisfies equation (2) (Figure 1). The physical meaning of equation (2) is obvious, points *F*, located such that time difference *|T(F,S) + T(R,F) – T(R,S)|* is smaller than one half of the period, will constructively interfere with wavefields at *R*, which serves as the base theory for claims that the resolution limit of travel-time tomography is the width of first Fresnel zone. Assuming the distance between source *S* and receiver *R* is *L* and wavelength of the propagating ultrasound signal is λ, the width of the first Fresnel zone is approximately $\sqrt{\lambda L}$ [1], which is often claimed as the resolution limit of the travel time tomography[2-10]. Although often used, this condition is not accurate when broadband signals are used. To better understand the limitation, we performed experiments as described below.
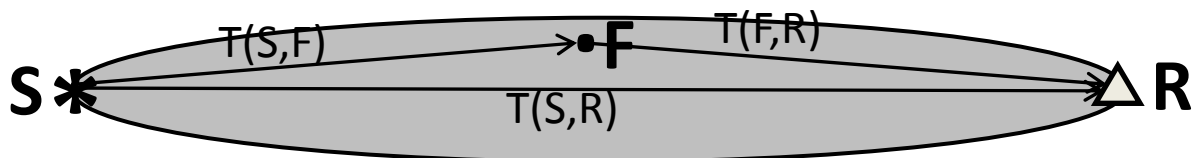
Figure 1.   Schematic plots of the first Fresnel zone.

2.3 Numerical simulations

In our simulations, the source-receiver geometry is ring shaped, modeled after our clinical prototype ultrasound scanner[15,16] designed for *in vivo* breast imaging. The diameter of the acquisition ring is 200 mm. Synthetic models with different anomaly sizes and velocity contrast were designed to test the resolving power of travel time tomography. Numerical acoustic wave propagation through these perturbation models was performed to generate synthetic data.   In these simulations, we used a broadband wavelet with a center frequency of 0.88 MHz as our acoustic source signal (Figure 2). The corresponding first Fresnel width at the center of ring for this source signal in Figure 2 is ~18 mm.
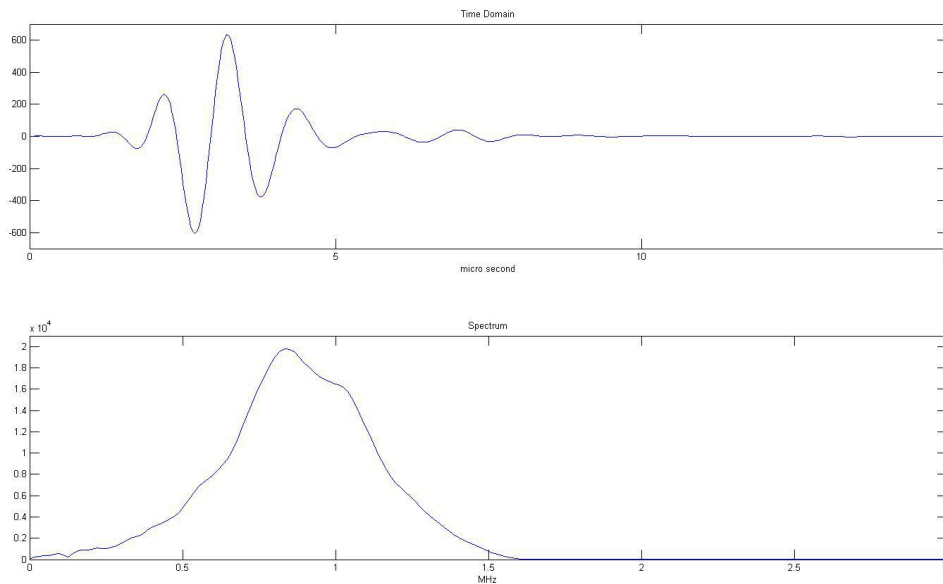
Figure 2.   Source wavelet and its spectrum used in the simulations.

Figures 3(a) and 3(b) are gray-scale representation of the true numerical models used in this study. For different simulations, the diameter of the anomalies in Fig. 2(a) and 2(b) can be 7.5 mm (~4.4 times the dominant wavelength), 6 mm (~3.5 times the dominant wavelength) or 5 mm (~3 times the dominant wavelength). Shortest distance between adjacent anomalies are always the same as the diameter of the corresponding anomalies. In

addition, the background sound speed in these models is 1.5 km/s while the anomalies have sound speeds of 1.515 km/s, 1.53 km/s or 1.55 km/s depending on the simulation. Using these numerical simulation, we investigated how travel time picking methods, ray coverage and data signal-to-noise ratio affect the resolving power of travel-time tomography. We also assessed the resolution limit of the bent-ray travel-time tomography.

(a)   (b)
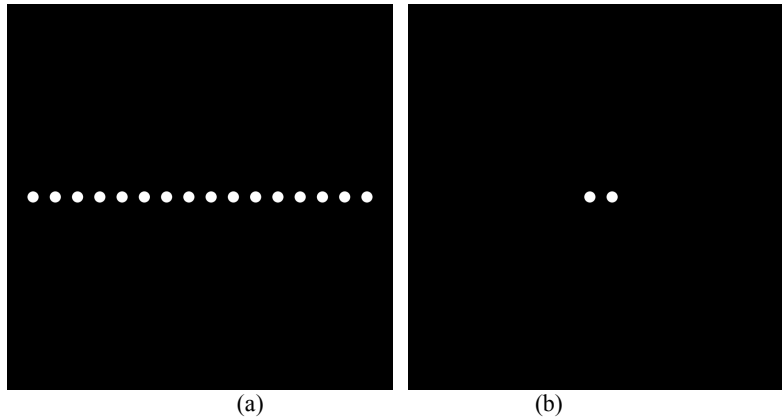
Figure 3. True numerical models.

3. RESULTS

We have tested a variety of factors that may affect the resolvability and detectability of bent-ray travel-time tomography. We further assess the resolution limit of the bent-ray travel-time tomography based on our AIC first arrival picks of numerical waveform data. Applications to in vitro and in vivo data are also presented here.

3.1 Effect of travel time picking methods

For noise-free data, accurate travel times could be picked for objects much smaller than the first Fresnel zone associated with the dominant frequency. In this study, two auto-picking schemes are used to consistently pick the first arrival travel times. One picking method is our in-house AIC picker[17] and the other one is the classic cross-correlation method. The major difference of these two methods can be summarized as follows: the AIC picker picks the first rise of the signal, while the cross-correlation method calculates the time shift of the prevailing signal relative to a known reference signal. A comparison of sound speed tomograms using our in-house AIC picker and using the cross correlation picker is illustrated in Fig. 4, where Figure 4(a) is reconstructed with our AIC travel time picks and Figure 4(b) is reconstructed with cross correlation travel time picks. Cross sections along the horizontal lines in Figure 4(a) and 4(b), overlaid with the true sound speed profile, are presented Figure 4(c). The true model for this comparison is shown in Figure 3(a) with diameter of 7.5 mm and sound speed of 1.53 km/s for the anomalies.
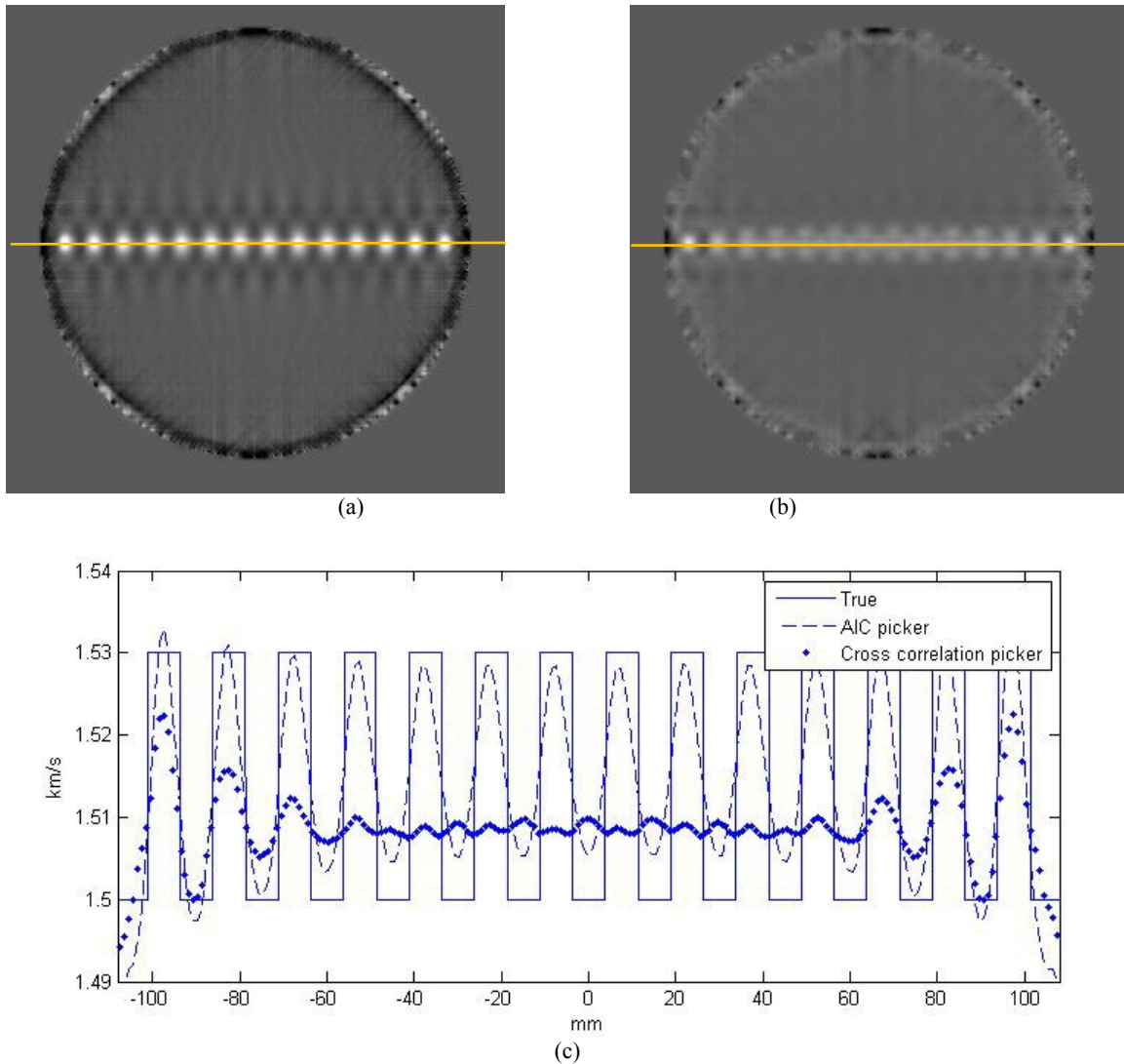
Figure 4. (a) Sound speed reconstruction with first arrival travel time picked using AIC picker. (b) Sound speed reconstruction with first arrival travel time picked using cross-correlation picker. (c) Cross-sections along the horizontal lines in (a) and (b) overlay with true profile. Solid line is the truth, dashed line is for the AIC picker and dotted line is for cross-correlation picker.

3.2 Effect of ray coverage

We compared sound speed reconstructions with different ray coverage (Figure 5) for the true model shown in Fig. 3(a) where anomalies have a diameter of 7.5 mm and a sound speed of 1.53 km/s. Figure 5(a), 5(b) and 5(c) are tomograms reconstructed with 128, 256 and 1024 acquisition elements, respectively. We also present the cross-section plots along the horizontal line (Figure 5(d)) and the vertical line (Fig. 5(e)). Although the inclusions can be detected in all three tomograms, the reconstructed images become noisier when fewer elements are used to acquire data, mainly due to the lack of adequate ray coverage.
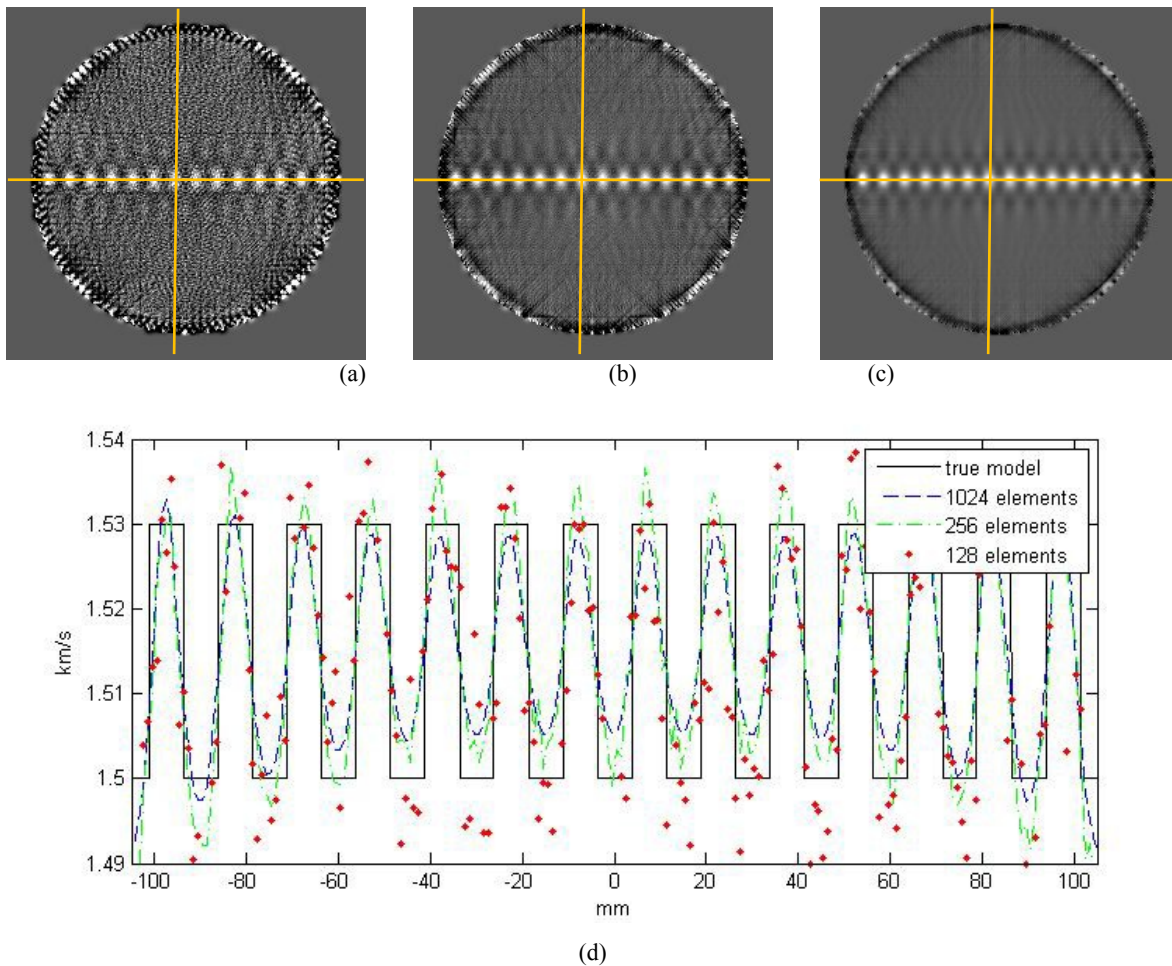
Figure 5. (a) Sound speed reconstruction with 128 acquisition elements. (b) Sound speed reconstruction with 256 acquisition elements. (c) Sound speed reconstruction with 1024 acquisition elements. (d) Cross-section plots along the horizontal lines in (a), (b) and (c). (e) Cross-section plots along the vertical lines in (a), (b) and (c). Solid line is the truth, dashed line is for 1024 elements, dash dotted line is for 256 elements and dotted line is for 128 elements.

3.3 Effect of signal-to-noise ratio (SNR)

When realistic noise is introduced in the waveform data, travel time picking of individual traces becomes less accurate, which, consequently, will affect the ability to resolve or detect small objects. We used the true model in Figure 3(b) with anomaly diameter of 7.5 mm and sound speed of 1.515 km/s to demonstrate how noise affects the resolvability and detectability of bent-ray travel time tomography. We gradually increased the level of random noise added to the synthetic waveforms from 10% to 30% then to 70% of the average amplitude of the original noise-free waveforms. The corresponding sound speed images are presented from Figure 6(a) through 6(c). The cross-section plots along the horizontal lines in Figure 6(d) clearly show the decreasing resolvability and detectability of the travel-time tomography with decreasing SNR.
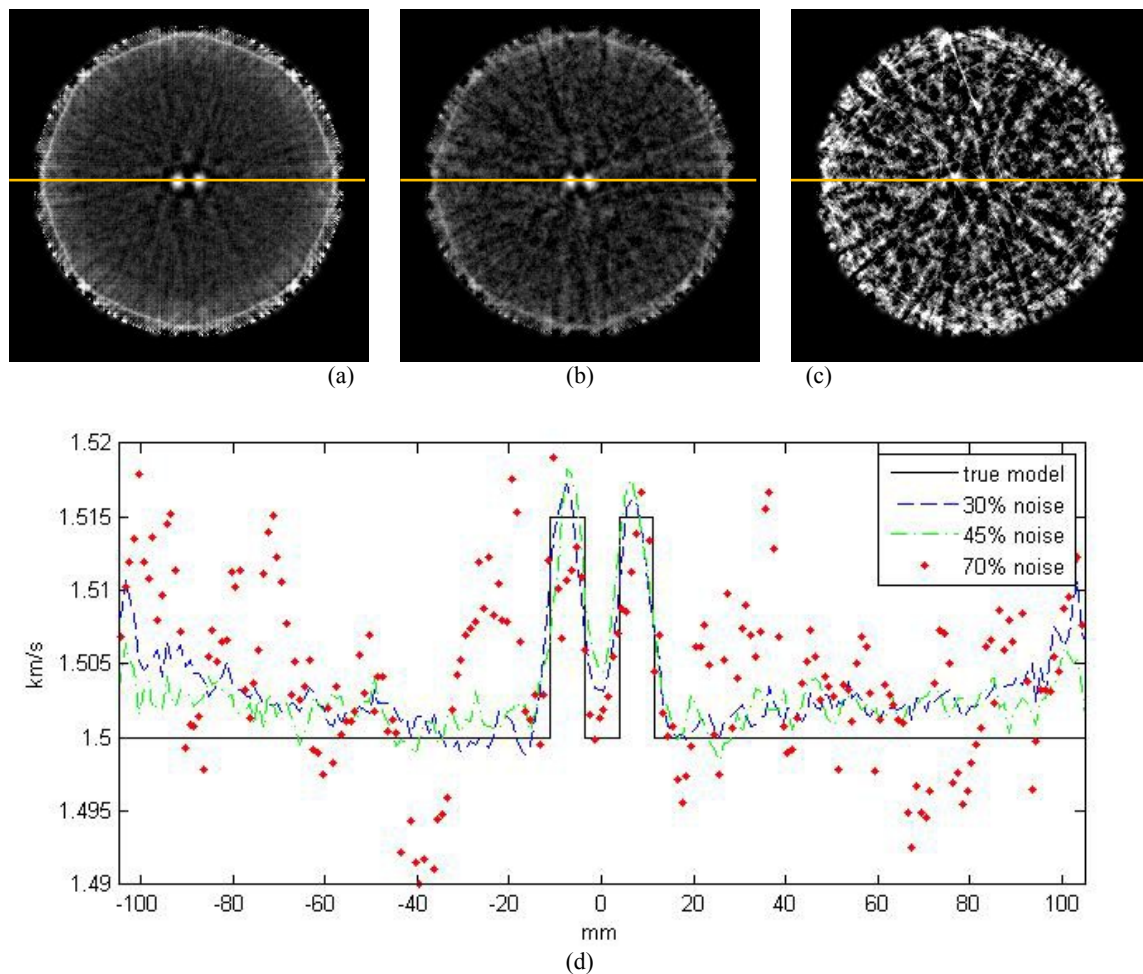
Figure 6. Effect of noise. (a) Sound speed reconstruction with added noise of 10% of the average amplitude of the original noise-free waveforms.   (b) Same as (a) but with a noise level of 30% of the average amplitude of the original noise-free waveforms. (c) Same as (a) but with a noise level of 30% of the average amplitude of the original noise-free waveforms. (d) Cross-section plots along the horizontal lines in (a), (b) and (c). Solid line is the truth, dashed line is for 10% added noise, dash dotted line is for 30% added noise and dotted line is for 70% added noise.

3.4 Resolution limit of bent-ray travel time tomography

As shown in the above simulations, the resolution limit of bent-ray travel-time tomography is much better than the well cited first Fresnel zone for broadband signals. To further verify this point, we performed a series of simulations with numerical models of different anomaly sizes and different separations. Schematic plots of the true models in this test are shown in Figure 3(b). Anomaly sizes used in our simulations are 7.5 mm (~4.4 wavelengths), 6 mm (~3.5 wavelengths) and 5 mm (~3 wavelengths). The separations between the two anomalies are the same as their diameters. 1.55 km/s (3.3%) sound speed contrast to 1.5 km/s background and 1024 acquisition elements are used in these simulations. The reconstructed sound speed images are presented in Figure 7(a) through 7(c). The corresponding cross-section profiles along the horizontal lines are shown in Figure 7(d) through 7(f). For the model with anomaly size and anomaly distance of ~4.4 wavelengths (Figure 7(a) and 7(d)) the true sound speed contrast are well resolved at the centers of each anomaly. It is obvious that the resolvability is degraded when the anomaly size and distance get smaller. However, for anomaly sizes as small as 5 mm (~3 wavelengths), we still can detect both the anomalies in the reconstructions.
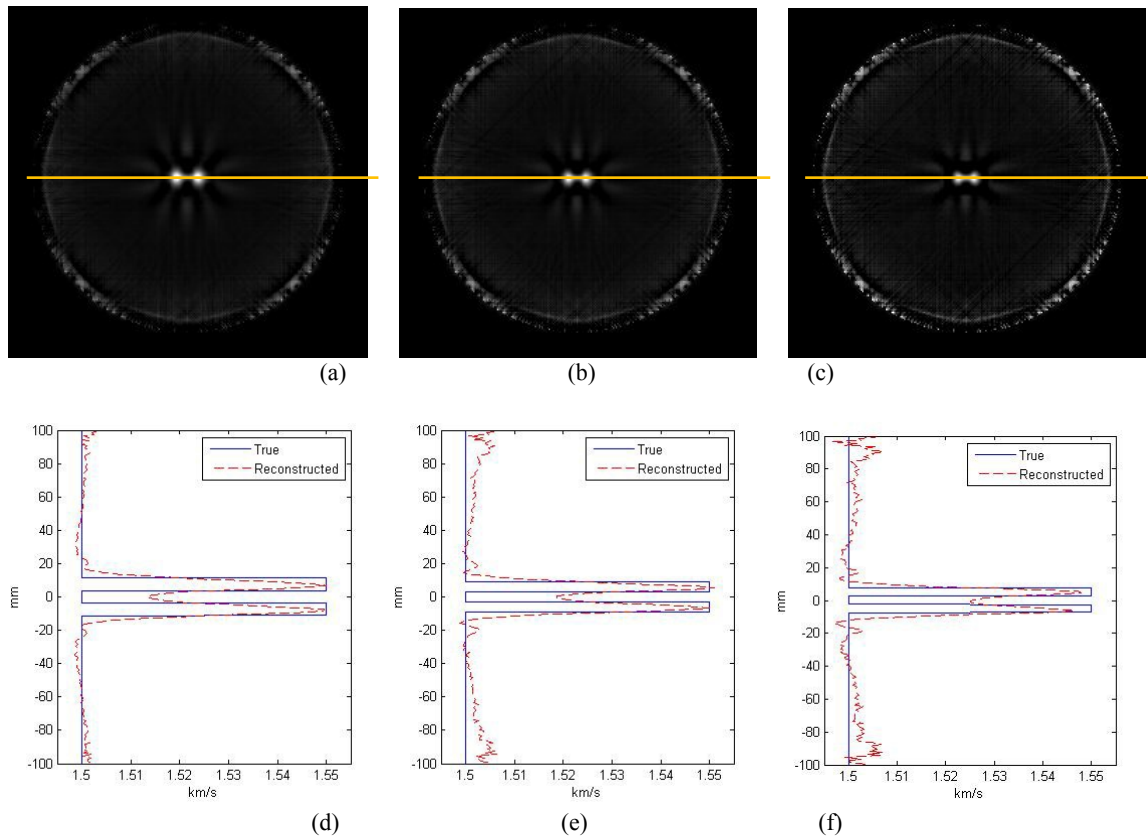
Figure 7. Assessment of resolution limit of bent-ray travel time tomography (a) Sound speed reconstruction anomaly diameter of 7.5 mm (~4.4 wavelengths) and nearest distance between the two anomalies is also 7.5 mm. (b) Sound speed reconstruction anomaly diameter of 6 mm (~3.5 wavelengths) and nearest distance between the two anomalies is also 6 mm. (c) Sound speed reconstruction anomaly diameter of 5 mm (~3 wavelengths) and nearest distance between the two anomalies is also 5 mm. (d) Cross-section plots along the horizontal lines in (a). (e) Cross-section plots along the horizontal lines in (b). (f) Cross-section plots along the horizontal lines in (c). Solid line is the truth, dashed line is the reconstructed profile.

4. DISCUSSION AND CONCLUSIONS

The first Fresnel zone associated with the dominant frequency is commonly cited in the literature as the resolution limit of travel-time tomography[2-10]. However, our study shows that the first Fresnel zone is too conservative as a resolution estimate for travel-time tomography. The resolving power of the bent-ray travel-time tomography is usually beyond the first Fresnel zone and determined by a lot of factors, and the wave front healing[2] is not the dominant factor to determine the resolution. In this paper, we investigate factors that affect the resolvability and detectability of the bent-ray travel-time tomography algorithm. Using the source signal in Fig. 1, we conduct simulations on different numerical models to test the effects of travel time picking method, ray coverage, combination of anomaly size and sound speed contrast, and data SNR on the resolving power of the algorithm. We will discuss each factor in detail in the following paragraphs.

As we shown in Figure 5, ray coverage greatly affects the resolving power of the bent-ray travel-time tomography. Travel-time tomography performs a weighted averaging of the picked first arrivals through the overlap of ray paths, so denser ray coverage will improve the resolvability and detectability of small objects that may be buried in noise in images reconstructed with sparse ray coverage. For circular acquisition system, rays are unevenly distributed – denser towards the center of the transducer ring and sparser towards the edge.

Undoubtedly, the noise level in the waveform data is one of the major contributing factors to the resolution limit of the bent-ray travel-time tomography. From simulations in Figure 6, we can clearly see that image resolution decreases with decreasing SNR. However, with noise level at 30% of the average amplitude of the original noise-free waveforms, the bent-ray travel-time tomography is still able to resolve the two anomalies whose size (7.5 mm) is less than half of the first Fresnel zone (~18 mm). When SNR drops to a certain level (Figure 6(c)), travel-time tomography cannot resolve the anomalies anymore. This is true for all tomography methods.

Our assessments on the resolution limit of bent-ray travel-time tomography based on numerical simulation show that the resolving power of bent-ray travel-time tomography is way beyond the width of the first Fresnel zone (~18 mm at the center of the ring in our case). In our simulations, anomaly size of 7.5 mm (~4.4 wavelengths) can be well resolved by bent-ray travel- time tomography (Figure 7(a) and 7(d)). Even for anomaly size of 3 wavelengths, the two inclusions at center of the acquisition ring are fairly resolved. From Figure 7, we can see the resolving power of the algorithm is decreasing with decreasing anomaly size.

In summary, there are many factors affecting the resolvability and detectability of bent-ray travel-time tomography including accuracy of first arrival travel time picks, ray coverage, combination of sound speed contrast and anomaly size, and data SNR. In this paper, we performed simulations to assess the effect of each factor on the resolving power of bend-ray travel-time tomography. Our simulations show that the with accurate first arrival travel time picks, enough ray coverage and good enough SNR, the resolving power of bent-ray travel-time tomography is much better than the width of the first Fresnel zone. The bent-ray travel-time tomography is even able to detect anomaly of ~3 wavelenths in diameter.

REFERENCES:

1. V. Cerverny, "Seismic Ray Theory," Cambridge University Press, 2001.

2. G. Nolet, "Seismic wave propagation and seismic tomography," Seismic Tomography, edited by G. Nolet, pp. 1-23, D. Reidel, Norwell, Mass, 1987.

3. G. Schuster, "Resolution limits for crosswell migration and traveltime tomography," Geophys. J. Int., 127, 427-440, 1996.

4. R. Snieder and A. Lomax, "Wavefield smoothing and the effect of rough velocity perturbations on arrival times and amplitudes," Geophys. J. Int., 125, 796-812, 1996.

5. G. Schuster, "Resolution limits for crosswell migration and traveltime tomography," Geophys. J. Int., 127, 427-440, 1996.

6. R. Pratt, "Seismic waveform inversion in the frequency domain. I. Theory and verification in a physical scale model," Geophysics, 64, 888-901, 1999.

7. S. Hung, F, Dahlen, and G. Nolet, "Wavefrong healing: a bnana-doughnut perspective," Geophys. J. Int., 146, 289-312, 2001.

8. J. Spetzler, C. Sivaji, O. Nishizawa and Y. Fukushima, " A test of ray theory and scattering theory based on a laboratory experiment using ultrasonic waves and numerical simulation by finite-difference method, " Geophys. J. Int., 148, 165-178, 2002.

9. J. Sheng and G. T. Schuster, "Finite-frequency resolution limits of traveltime tomography for smoothly varying velocity model," Geophys. J. Int., 152, 669-676, 2003.

10. P. Huthwaite and F. Simonetti, "High-resolution imaging without iteration: A fast and robust method for breast ultrasound tomography," J. Acoust. Soc. Am.,130, 1721-1734, 2011.

11. W. C. Pritchett, "Acquiring Better Seismic Data,", Chapman and Hall, New York, NY, 1990.

12. P. Williamson, "A guide to the limits of resolution imposed by scattering in ray tomography," Geophysics, 56, 202-207, 1991.

13. C. Li, N. Duric, N., "In vivo breast sound-speed imaging with ultrasound tomography," Ultrasound in Med. &

Biol., 35, 1615-1628, 2009.

14. Y. A., Kravtsov and Y. I. Orlov, "Geometrical optics of inhomogeneous media," Nauka, Moscow, 1980.

15. N. Duric, and P. Littrup, A. Babkin, D. Chambers, S. Azevedo, R. Pevzner, M. Tokarev, E. Holsapple, O. Rama, and R. Duncan, "Development of ultrasound tomography for breast imaging: Technical assessment," Medical Physics, 32, 1375-1386, 2005.

16. N. Duric, and P. Littrup, L. Poulo, A. Babkin, R. Pevzner, E. Holsapple, and O. Rama, "Detection of Breast Cancer With Ultrasound Tomography: First Results with the Computerized Ultrasound Risk Evaluation (C.U.R.E) Prototype," Medical Physics, 34, 773-785, 2007.

17. C. Li , L. Huang, N. Duric, H. Zhang and C. Rowe, "An improved automatic time-of-fight picker for medical ultrasound tomography," Ultrasonics, 49, 61-72, 2009.